SOLUTION OF BOUNDARY INTEGRAL EQUATIONS FOR EDDY CURRENT NONDESTRUCTIVE EVALUATION IN THREE DIMENSIONS

Ming Yang, Jiming Song, and Norio Nakagawa

Citation: AIP Conf. Proc. **1096**, 303 (2009); doi: 10.1063/1.3114219
View online: http://dx.doi.org/10.1063/1.3114219
View Table of Contents: http://proceedings.aip.org/dbt/dbt.jsp?KEY=APCPCS&Volume=1096&Issue=1
Published by the American Institute of Physics.

SOLUTION OF BOUNDARY INTEGRAL EQUATIONS FOR EDDY CURRENT NONDESTRUCTIVE EVALUATION IN THREE DIMENSIONS

Ming Yang [1, 2], Jiming Song [2], and Norio Nakagawa [1]

[1] Center for Nondestructive Evaluation, Iowa State University, Ames, IA 50011
[2] Department of Electrical and Computer Engineering, Iowa State University, Ames, IA 50011

ABSTRACT: Eddy current nondestructive evaluation (NDE) of airframe structures involves the detection of electromagnetic field irregularities due to non-conducting inhomogeneities in an electrically conducting material, which often treats with complicated geometrical features such as cracks, fasteners, sharp corners/edges, multi-layered structures, etc. The eddy-current problem can be formulated by the boundary integral equations (BIE) and discretized into matrix equations by the method of moments (MoM) or the boundary element method (BEM). This paper introduces the implementation of Stratton-Chu formulation for the conductive medium, in which the induced electric and magnetic surface currents are expanded in terms of Rao-Wilton-Glisson (RWG) vector basis function and the normal component of magnetic field is expanded in terms of pulse basis function. Also, a low frequency approximation is applied in the external medium, that is, free space in our case. Computational tests are presented to demonstrate the accuracy and capability of the BIE method with a complex wave number for three-dimensional objects described by a number of triangular patches. This work prepares the BIE solution procedure that will be embedded with the Fast Multipole Method (FMM), which is a well-established and effective method for accelerating numerical solutions of the matrix equations. When accelerated by the FMM, the BIE method will have the capability of solving large-scale electromagnetic wave propagation and eddy-current problems.

Keywords: Boundary Integral Equation, Eddy Current
PACS: 41.20.Cv, 81.70.Ex

INTRODUCTION

Eddy current nondestructive evaluation (NDE) involves the detection of electromagnetic field irregularities due to non-conducting inhomogeneities in an electrically conducting material [1]. Certain eddy-current modeling such as NDE of airframe structures often treats with complicated geometrical features such as cracks, fasteners, sharp corners/edges, multi-layered structures, etc. Typically, the primary eddy current field is produced by sinusoidal excitation of a small induction coil near the surface of the component to be inspected. With scanning the coil over the surface, the

CP1096, *Review of Quantitative Nondestructive Evaluation Vol. 28,*
edited by D. O. Thompson and D. E. Chimenti

flaw detection is achieved by searching for coil impedance changes that imply flaw-induced perturbation of the eddy current density [2]. Therefore, computer simulation of the flaw detection process includes calculation of the electromagnetic field distribution around the flaw and the response of the detection system to this perturbed distribution.

In what follows, we introduce a boundary integral equation (BIE) method for the eddy current NDE in three dimensions. The problem can be formulated by the BIE and discretized into matrix equations by the method of moments (MoM) or the boundary element method (BEM) [3-4]. As we demonstrate an implementation of the Stratton-Chu formula [5] for the conductive medium, the induced electric and magnetic surface currents are expanded in terms of Rao-Wilton-Glisson (RWG) vector basis function [6] while the normal component of magnetic field is expanded in terms of the pulse basis function. Also, a low frequency approximation is applied in the external medium, that is, free space in our case. Computational tests are presented to demonstrate the accuracy and capability of the three-dimensional BIE method with a complex wave number for arbitrarily shaped objects described by a number of triangular patches. The results of this paper set the stage for the BIE method to be embedded with the Fast Multipole Method (FMM) [7-8], which is a well-established and effective method for accelerating numerical solutions of the matrix equations. When accelerated by the FMM, the BIE method will have the capability of solving large-scale electromagnetic wave propagation and eddy-current problems [9-10].

FORMULATION

We start with the version of the Stratton-Chu formulas [5], which explicitly contains the normal components of the surface fields

$$\mathbf{E}(\mathbf{r}) = \mathbf{E}^{inc}(\mathbf{r}) + \int_S \left[i\omega\mu G(\mathbf{r},\mathbf{r}')(\hat{\mathbf{n}}\times\mathbf{H}(\mathbf{r}')) + (\hat{\mathbf{n}}\cdot\mathbf{E}(\mathbf{r}'))\nabla' G(\mathbf{r},\mathbf{r}') + (\hat{\mathbf{n}}\times\mathbf{E}(\mathbf{r}'))\times\nabla' G(\mathbf{r},\mathbf{r}') \right] dS' \quad (1)$$

$$\mathbf{H}(\mathbf{r}) = \mathbf{H}^{inc}(\mathbf{r}) + \int_S \left[-i\omega\varepsilon G(\mathbf{r},\mathbf{r}')(\hat{\mathbf{n}}\times\mathbf{E}(\mathbf{r}')) + (\hat{\mathbf{n}}\cdot\mathbf{H}(\mathbf{r}'))\nabla' G(\mathbf{r},\mathbf{r}') + (\hat{\mathbf{n}}\times\mathbf{H}(\mathbf{r}'))\times\nabla' G(\mathbf{r},\mathbf{r}') \right] dS' \quad (2)$$

where S is the boundary of the interest domain, $\mathbf{r},\mathbf{r}' \in S$ are the source and field points, respectively, and $G_j(\mathbf{r},\mathbf{r}') = e^{ik_j|\mathbf{r}-\mathbf{r}'|}/(4\pi|\mathbf{r}-\mathbf{r}'|)$, $k_j^2 = \omega^2\mu_j\varepsilon_j$, $j = 1,2$, $\hat{\mathbf{n}}$ is the unit normal direction pointing towards solution domain. These formulas provide stable solutions at low frequencies as they remain valid even in the static limit.

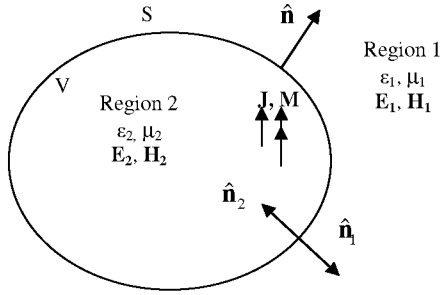

FIGURE 1. Field geometry inside and outside a closed surface S, where the outside (Region 1) is free space and the inside (Region 2) is a conductive medium.

Then, we may write down formulas in the region 1 and the region 2, as shown in Figure 1, when the angular frequency ω approaches to zero. For the region 1, since $\hat{\mathbf{n}}_1 = \hat{\mathbf{n}}$ and $\nabla' G_1(\mathbf{r},\mathbf{r}') = -\nabla G_1(\mathbf{r},\mathbf{r}')$, equation (2) can be written as:

$$\mathbf{H}_1(\mathbf{r}) \approx \mathbf{H}^{inc}(\mathbf{r}) + \int_S \left[-\frac{1}{\mu_1} \nabla G_1(\mathbf{r},\mathbf{r}')(\hat{\mathbf{n}} \bullet \mathbf{B}(\mathbf{r}')) + \nabla G_1(\mathbf{r},\mathbf{r}') \times (\hat{\mathbf{n}} \times \mathbf{H}(\mathbf{r}')) \right] dS' \tag{3}$$

For the region 2, since $\hat{\mathbf{n}}_2 = -\hat{\mathbf{n}}$ and $\nabla' G_2(\mathbf{r},\mathbf{r}') = -\nabla G_2(\mathbf{r},\mathbf{r}')$, equation (1) and (2) can be written as:

$$\begin{aligned} \mathbf{E}_2(\mathbf{r}) &= \int_S \left[-i\omega\mu_2 G_2(\mathbf{r},\mathbf{r}')(\hat{\mathbf{n}} \times \mathbf{H}(\mathbf{r}')) + \nabla G_2(\mathbf{r},\mathbf{r}'))(\hat{\mathbf{n}} \bullet \mathbf{E}(\mathbf{r}')) + (-\nabla G_2(\mathbf{r},\mathbf{r}')) \times (\hat{\mathbf{n}} \times \mathbf{E}(\mathbf{r}')) \right] dS' \\ &\approx -\int_S \left[i\omega\mu_2 G_2(\mathbf{r},\mathbf{r}')(\hat{\mathbf{n}} \times \mathbf{H}(\mathbf{r}')) + \nabla G_2(\mathbf{r},\mathbf{r}') \times (\hat{\mathbf{n}} \times \mathbf{E}(\mathbf{r}')) \right] dS' \end{aligned} \tag{4}$$

$$\mathbf{H}_2(\mathbf{r}) = \int_S \left[i\omega\varepsilon_2 G_2(\mathbf{r},\mathbf{r}')(\hat{\mathbf{n}} \times \mathbf{E}(\mathbf{r}')) + \frac{1}{\mu_2} \nabla G_2(\mathbf{r},\mathbf{r}')(\hat{\mathbf{n}} \bullet \mathbf{B}(\mathbf{r}')) - \nabla G_2(\mathbf{r},\mathbf{r}') \times (\hat{\mathbf{n}} \times \mathbf{H}(\mathbf{r}')) \right] dS' \tag{5}$$

where $\varepsilon_2 = \varepsilon_0 \varepsilon_{r2} + i\sigma/\omega \approx i\sigma/\omega$, $\hat{\mathbf{n}} \bullet \mathbf{E}_2 = \hat{\mathbf{n}} \bullet (\varepsilon_1 \mathbf{E}_1 / \varepsilon_2) << 1$, and at the interface, $\hat{\mathbf{n}} \bullet \mathbf{B}_1 = \hat{\mathbf{n}} \bullet \mathbf{B}_2 \Leftrightarrow \hat{\mathbf{n}} \bullet \mu_1 \mathbf{H}_1 = \hat{\mathbf{n}} \bullet \mu_2 \mathbf{H}_2$. If the region 1 is defined as free space,

$$G_1(\mathbf{r},\mathbf{r}') = e^{i\sqrt{k_0^2 + i\omega\mu_0\sigma}|\mathbf{r}-\mathbf{r}'|} \Big/ (4\pi|\mathbf{r}-\mathbf{r}'|) = e^{ik_0|\mathbf{r}-\mathbf{r}'|} \Big/ (4\pi|\mathbf{r}-\mathbf{r}'|) \approx 1/(4\pi|\mathbf{r}-\mathbf{r}'|)$$

To make the equations more compact, we introduce equivalent surface currents $\bar{\mathbf{J}}_S(\mathbf{r}) = \hat{\mathbf{n}} \times \bar{\mathbf{H}}(\mathbf{r})$, $\mathbf{M}_S(\mathbf{r}) = \mathbf{E}(\mathbf{r}) \times \hat{\mathbf{n}}$, with $\bar{\mathbf{H}}(\mathbf{r}) = \eta_1 \mathbf{H}(\mathbf{r}) = \sqrt{\mu_1/\varepsilon_1}\,\mathbf{H}(\mathbf{r})$. Additionally, equations (3) and (5) are multiplied by $\eta_1 = \sqrt{\mu_1/\varepsilon_1}$ to balance the MoM matrix; therefore, the three chosen Stratton-Chu formulas can be written as:

$$\eta_1 \mathbf{H}_1(\mathbf{r}) \approx \eta_1 \mathbf{H}^{inc}(\mathbf{r}) + \int_S \left[-\frac{1}{\sqrt{\mu_1\varepsilon_1}} \nabla G_1(\mathbf{r},\mathbf{r}')(\hat{\mathbf{n}} \bullet \mathbf{B}(\mathbf{r}')) + \nabla G_1(\mathbf{r},\mathbf{r}') \times \bar{\mathbf{J}}_S(\mathbf{r}') \right] dS' \tag{6}$$

$$\mathbf{E}_2(\mathbf{r}) \approx -\int_S \left[i\frac{k_2\eta_2}{\eta_1} G_2(\mathbf{r},\mathbf{r}')(\bar{\mathbf{J}}_S(\mathbf{r}')) - \nabla G_2(\mathbf{r},\mathbf{r}') \times \mathbf{M}_S(\mathbf{r}') \right] dS' \tag{7}$$

$$\eta_1 \mathbf{H}_2(\mathbf{r}) = \int_S \left[-i\frac{k_1\varepsilon_2}{\varepsilon_1} G_2(\mathbf{r},\mathbf{r}')\mathbf{M}_S(\mathbf{r}') + \frac{\eta_1}{\mu_2} \nabla G_2(\mathbf{r},\mathbf{r}')(\hat{\mathbf{n}} \bullet \mathbf{B}(\mathbf{r}')) - \nabla G_2(\mathbf{r},\mathbf{r}') \times \bar{\mathbf{J}}_S(\mathbf{r}') \right] dS' \tag{8}$$

Letting the observation point $\mathbf{r}$ approach surface S and then taking the cross product of equations (6) and (7) and the dot product of equation (8) with $\hat{\mathbf{n}}$ yields:

$$\frac{1}{2}\bar{\mathbf{J}}_S(\mathbf{r}) + \hat{\mathbf{n}} \times \mathbf{R}_1(\tilde{B}_n) - \hat{\mathbf{n}} \times \mathbf{K}_1(\bar{\mathbf{J}}_S) \approx \hat{\mathbf{n}} \times \eta_1 \mathbf{H}^{inc}(\mathbf{r}) \tag{9}$$

$$\frac{1}{2}\mathbf{M}_S(\mathbf{r}) - ik_1 \frac{\mu_2}{\mu_1} \hat{\mathbf{n}} \times \mathbf{L}_2(\bar{\mathbf{J}}_S) + \hat{\mathbf{n}} \times \mathbf{K}_2(\mathbf{M}_S) \approx 0 \tag{10}$$

$$\frac{1}{2}\tilde{B}_n + ik_1 \frac{\varepsilon_2\mu_2}{\varepsilon_1\mu_1} \hat{\mathbf{n}} \bullet \mathbf{L}_2(\mathbf{M}_S) + \frac{\mu_2}{\mu_1} \hat{\mathbf{n}} \bullet \mathbf{K}_2(\bar{\mathbf{J}}_S) - \hat{\mathbf{n}} \bullet \mathbf{R}_2(\tilde{B}_n) = 0 \tag{11}$$

where $\tilde{B}_n$ is defined as $\tilde{B}_n = \hat{\mathbf{n}} \bullet \mathbf{B}(\mathbf{r}) \big/ \sqrt{\mu_1\varepsilon_1}$ and the operators $\mathbf{L}$, $\mathbf{K}$, and $\mathbf{R}$ are defined as follows:

$$\mathbf{L}_j(\mathbf{X}) = \int_S \left[G_j(\mathbf{r},\mathbf{r}')\mathbf{X}(\mathbf{r}') \right] dS' \tag{12}$$

$$\mathbf{K}_j(\mathbf{X}) = P.V. \int_S \nabla G_j(\mathbf{r},\mathbf{r}') \times \mathbf{X}(\mathbf{r}') dS' \tag{13}$$

$$\mathbf{R}_j(\mathbf{X}) = \text{P.V.} \int_S \nabla G_j(\mathbf{r},\mathbf{r}')(\hat{\mathbf{n}}'\bullet\mathbf{X}(\mathbf{r}'))dS' = \text{P.V.} \int_S \nabla G_j(\mathbf{r},\mathbf{r}')X_n(\mathbf{r}')dS' \tag{14}$$

MOM IMPLEMENTATION

Firstly, using RWG basis of $\mathbf{\Lambda}_n(\mathbf{r})$ [6], which is curl-free and divergence-conforming, the induced currents are expanded as:

$$\overline{\mathbf{J}}_S(\mathbf{r}) = \sum_{n=1}^{N_e} a_n \mathbf{\Lambda}_n(\mathbf{r}),\ \mathbf{M}_S(\mathbf{r}) = \sum_{n=1}^{N_e} c_n \mathbf{\Lambda}_n(\mathbf{r}), \tag{15}$$

where N_e is the total edge number. The structure of RWG basis function is similar to a roof-top basis function and its value comes from the fact that it eliminates line charges at edges. Using pulse basis $b_n(\mathbf{r})$ for triangular mesh T_n, the normal component of magnetic field is expanded as:

$$\tilde{B}_n = \hat{\mathbf{n}}\bullet\mathbf{B}(\mathbf{r})\Big/\sqrt{\mu_1\varepsilon_1} = B_n\Big/\sqrt{\mu_1\varepsilon_1} = \sum_{n=1}^{N_p} d_n b_n(\mathbf{r}), \tag{16}$$

where $b_n(\mathbf{r}) = \begin{cases} 1 & \mathbf{r}\in T_n \\ 0 & otherwise \end{cases}$ and N_p is the total patch number.

Secondly, using Galerkin's method, equations (9) and (10) can be tested with $\mathbf{\Lambda}_m(\mathbf{r})$ and equation (11) tested with $b_m(\mathbf{r})$. Then, discretized matrix equations are formed by means of numerical integration rule, $\frac{1}{T}\int_T dS\ f(\mathbf{r}) = \sum_{g=1}^{N_g} W_g f(\mathbf{r}_g)$, in which N_g is the total integral point number in the patch.

Finally, the discretized MoM matrix of the Stratton-Chu formulas reads

$$\begin{bmatrix} \frac{1}{2}\mathbf{T}-\mathbf{K}_1^{\times} & 0 & \mathbf{R}_1^{\times} \\ -ik_1\frac{\mu_2}{\mu_1}\mathbf{L}_2^{\times} & \frac{1}{2}\mathbf{T}+\mathbf{K}_2^{\times} & 0 \\ \frac{\mu_2}{\mu_1}\mathbf{K}_2^{n} & ik_1\frac{\varepsilon_2\mu_2}{\varepsilon_1\mu_1}\mathbf{L}_2^{n} & \frac{1}{2}\mathbf{D}-\mathbf{R}_2^{n} \end{bmatrix} \begin{bmatrix} \mathbf{a} \\ \mathbf{c} \\ \mathbf{d} \end{bmatrix} = \begin{bmatrix} \mathbf{V}^I \\ 0 \\ 0 \end{bmatrix}$$

where the subscript $j=1,2$ stand for medium 1 or medium 2, and the superscript $\times$ and n denote the product of normal component of $\hat{\mathbf{n}}\times$ or $\hat{\mathbf{n}}$. Furthermore, the expanding terms in the MoM matrix are shown in the following:

$$T_{mn} = \int_{S_m} dS\ \mathbf{\Lambda}_m(\mathbf{r})\bullet\mathbf{\Lambda}_n(\mathbf{r})$$

$$D_{mn} = \int_{T_m} dS\ b_m(\mathbf{r})b_n(\mathbf{r}) = \delta_{mn}\int_{T_m} dS = \delta_{mn}T_m$$

$$K_{jmn}^{\times} = \int_{S_m} dS\ \left[\mathbf{\Lambda}_m(\mathbf{r})\times\hat{\mathbf{n}}\right]\bullet\left[\int_{S_n}\nabla G_j(\mathbf{r},\mathbf{r}')\times\mathbf{\Lambda}_n(\mathbf{r}')dS'\right]$$

$$K_{jmn}^{n} = \int_{T_m} dS\ b_m(\mathbf{r})\left[\hat{\mathbf{n}}\bullet\int_{S_n}\nabla G_j(\mathbf{r},\mathbf{r}')\times\mathbf{\Lambda}_n(\mathbf{r}')dS'\right]$$

$$L^{\times}_{jmn} = \int_{S_m} dS \ \left[\boldsymbol{\Lambda}_m(\mathbf{r})\times\hat{\mathbf{n}}\right]\bullet\left[\int_{S_n} G_j(\mathbf{r},\mathbf{r}')\boldsymbol{\Lambda}_n(\mathbf{r}')dS'\right]$$

$$L^{n}_{jmn} = \int_{T_m} dS \ b_m(\mathbf{r})\left[\hat{\mathbf{n}}\bullet\int_{S_n} G_j(\mathbf{r},\mathbf{r}')\boldsymbol{\Lambda}_n(\mathbf{r}')dS'\right]$$

$$R^{\times}_{jmn} = \int_{S_m} dS \ \left[\boldsymbol{\Lambda}_m(\mathbf{r})\times\hat{\mathbf{n}}\right]\bullet\left[\int_{T_n} \nabla G_j(\mathbf{r},\mathbf{r}')b_n(\mathbf{r}')dS'\right]$$

$$R^{n}_{jmn} = \int_{T_m} dS \ b_m(\mathbf{r})\left[\hat{\mathbf{n}}\bullet\int_{T_n} \nabla G_j(\mathbf{r},\mathbf{r}')b_n(\mathbf{r}')dS'\right]$$

$$V^{I}_{m} = \eta_1\int_{S_m} dS \ \boldsymbol{\Lambda}_m(\mathbf{r})\bullet\left[\hat{\mathbf{n}}\times\mathbf{H}^{inc}(\mathbf{r})\right]$$

NUMERICAL TESTS

We now proceed to solve the three-dimensional Stratton-Chu formulas using the BIE method for the conductive medium. As an illustration of the method, a conducting sphere model is chosen as an example of the eddy current problem. The sphere with a radius of 1 meter is represented by 3200 flat triangles and 4800 edges, and the average edge length is around 0.097 meter. For a plane wave incident from the direction of $(\theta_i = 0, \varphi_i = 0)$ and polarized in the horizontal or vertical direction [11], the computation results of scattered electric fields are shown in Figure 2, as the observation surface is 0.1 meter outside the sphere surface. In this case, the working frequency is 3 MHz and the conductivity of the sphere is 5×10^3 S/m. The computation results agree well with the Mie series solution [12] at plane wave incidence.

To simulate air core coils in the probe field modeling, a small electric current loop is put at the Z-axis, with the coordinate of (0.0, 0.0, 1.2 meter) and its loop surface parallel to the XY plane. The electric current loop can be treated as a magnetic dipole:

$$I_m l = -iS\omega\mu_0 I_0 = -i\pi a^2\omega\mu_0 I_0 = 1$$

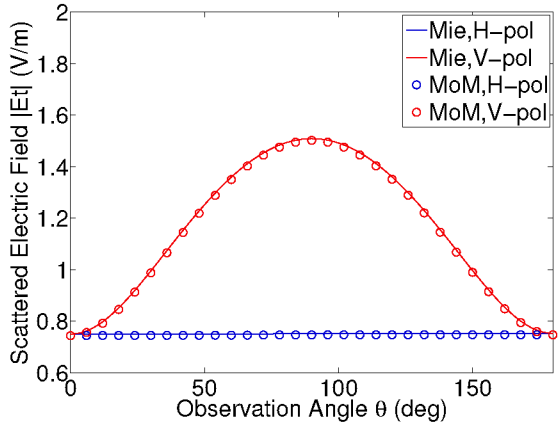

FIGURE 2. Comparison of scattered electric fields calculated by BIE method and those from Mie series solution for a conducting sphere with plane wave incidence. H-pol: horizontal polarization; V-pol: vertical polarization.

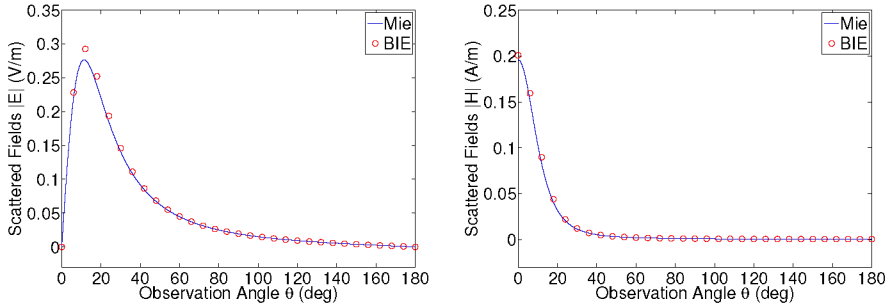

FIGURE 3. Comparison of scattered electric and magnetic fields calculated by BIE method and those from Mie series solution for a conducting sphere with localized magnetic dipole incidence.

The computation results of scattered electric and magnetic fields are shown in Figure 3, as the observation surface is 0.1 meter outside the sphere surface, with the frequency of 3 MHz and the sphere conductivity of 5×10^3 S/m. The solutions of scattered electric and magnetic fields reasonably agree with the Mie series solution with localized magnetic dipole incidence.

Furthermore, a cube model with the conductivity of 5×10^3 S/m is set as another example of the eddy current problem. The cube with a side length of 1 meter is represented by 1200 flat triangles and 1800 edges, and the average edge length is around 0.11 meter. The center of the cube is at the origin (0.0, 0.0, 0.0) and the magnetic dipole is put above the top surface of the cube at Z=0.7 m plane, as shown in Figure 4.

Figure 5 shows the snapshots of total time-harmonic electric field pattern at a 2m by 2m square in Z=0.6 m plane, as the magnetic dipole at a excitation frequency of 3 MHz moves towards a corner of the cube, as shown in Figure 4, which stands for a top surface scanning for the cube with a lift-off distance of 0.2 m. We present the vector plot of the in-phase components (denoted as $t=0$) and the quadrature components ($t=T/4$, where T is the period of the incident wave) separately. Each arrow in the figure is drawn from the point at which the electric field is evaluated, with length proportional to the magnitude of the vector at that point. These computation results have reasonable physical meanings for the primary eddy current field produced by sinusoidal excitation of a small induction coil in the cube model.

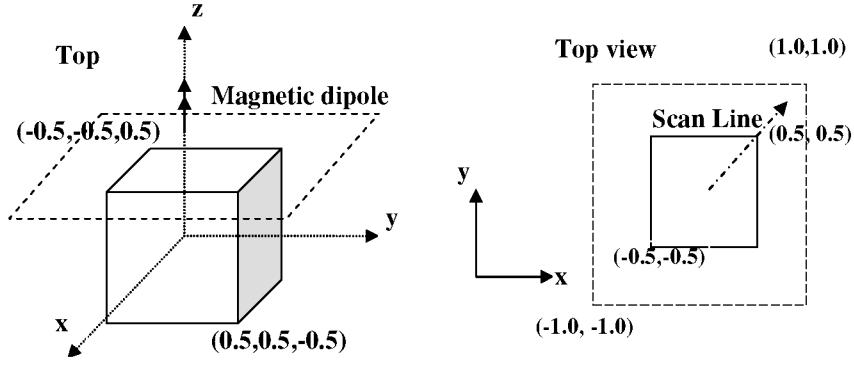

FIGURE 4. A conducting cube model and its top surface scanning diagram.

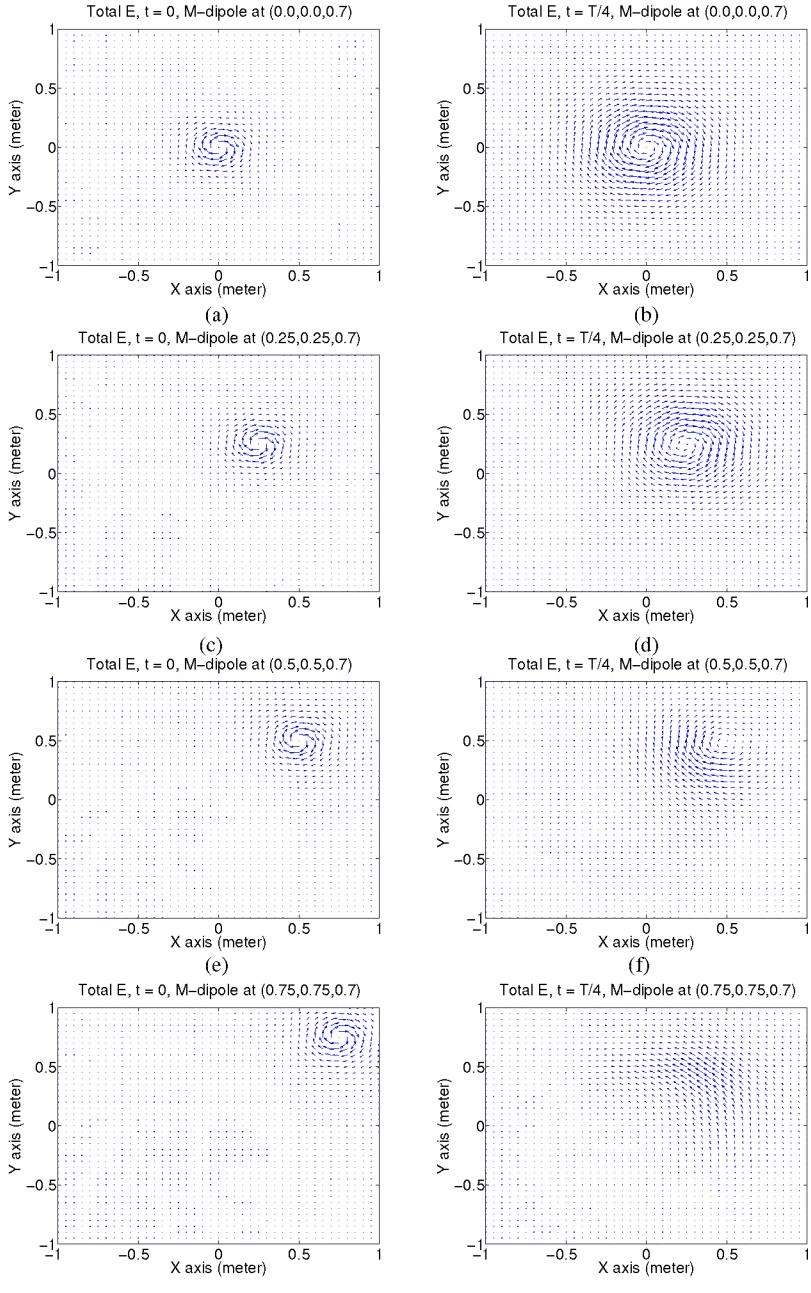

FIGURE 5. Snapshots of total time-harmonic electric field pattern at a 2m by 2m square in Z=0.6 m plane, as the magnetic dipole moves towards a corner of the cube. The labels $t=0$ and $t=T/4$ stand for the in-phase and quadrature components, respectively.

CONCLUSION

In this paper, we introduce a boundary integral equation method for modeling the eddy current inspection in three dimensions. The problem can be formulated by the BIE and discretized into matrix equations by MoM or BEM. In our implementation of the Stratton-Chu formula for the conductive medium, the induced electric and magnetic surface currents are expanded in terms of RWG vector basis function, while the normal component of magnetic field is expanded in terms of the pulse basis function. Also, the low frequency approximation is applied in the external medium. Computational tests are presented to demonstrate the accuracy and capability of the three-dimensional BIE method with a complex wave number for both sphere and cube models described by a number of triangular patches for the simulation of eddy current inspection processes. We plan to accelerate the BIE method by the FMM, so that we will have the capability of solving large-scale electromagnetic wave propagation and eddy-current problems.

ACKNOWLEDGMENTS

This material is based upon work supported in part by the Federal Aviation Administration under Contract #DTFA03-98-D-00008, Delivery Order #0039 and performed at Iowa State University's Center for NDE as part of the Center for Aviation Systems Reliability program. The authors are grateful to Prof. W.C. Chew and his research group for providing Mie series solution for magnetic dipole.

REFERENCES

1. H.L. Libby, *Introduction to Electromagnetic Nondestructive Test Methods*, Wiley, New York, NY, 1971.
2. B.A. Auld, *Eddy-Current Characterization of Materials and Structures*, ASTM STP 722, edited by G. Birnbaum and G. Free, Philadelphia, PA 1981, pp. 332.
3. R.F. Harrington, *Field Computation by Moment Methods,* Macmillan, New York, 1965.
4. M. Yang, J.M. Song, and N. Nakagawa, *Review of Progress in Quantitative NDE*, Golden, CO, Proceedings vol. **27A**, pp. 305-312 (2007).
5. J.A. Stratton, *Electromagnetic Theory*, McGraw-Hill, New York, NY 1941.
6. S. Rao, D. Wilton, and A. Glisson, *IEEE Trans. Antennas Propagat.*, vol **30**, pp. 409-418 (1982).
7. V. Rokhlin, *J. Comput. Phys.,* vol. **86**, pp. 414-439 (1990).
8. R. Coifman, V. Rokhlin, and S. Wandzura, *IEEE Antennas Propagat. Mag.,* vol. **35**, no. 3, pp. 7-12 (1993).
9. J.M. Song, C.C. Lu, and W.C. Chew, *IEEE Trans. Antennas Propagat.*, vol.**45**, no.10, pp.1488-1493 (1997).
10. W.C. Chew, J. Jin, E. Michielssen, and J. Song, Eds., *Fast and Efficient Algorithms in Computational Electromagnetics,* Artech House, Norwood, MA, 2001.
11. M. Yang and J. M. Song, *IEEE AP-S International Symposium*, Albuquerque, NM, pp. 2873-2876 (2006).
12. R.F. Harrington, Time Harmonic Electromagnetic Fields, McGraw-Hill, New York, NY, section 6-9, 1961.